

New HERA Results on Diffraction

S. Levonian

DESY, Notkestraße 85, 22607 Hamburg, Germany

Abstract

Four new measurements are presented from the area of diffractive and exclusive production at HERA. Preliminary results are available for isolated photons in diffractive photoproduction from ZEUS and open charm cross section in diffractive deep-inelastic scattering (DIS) regime from H1. ZEUS Collaboration has also measured the cross-section ratio $\sigma_{\psi(2S)}/\sigma_{J/\psi(1S)}$ in exclusive DIS using full HERA data statistics. Finally, H1 Collaboration for the first time studied exclusive ρ^0 meson photoproduction associated with a leading neutron at HERA.

Keywords: diffraction, HERA, exclusive reactions, isolated photons, diffractive charm, leading neutrons

1. Introduction

Diffraction is an important and challenging part of physics landscape at the electron-proton collider HERA. It represents a complicated interplay of soft and hard phenomena, thus providing rich opportunities for QCD studies. Diffractive ep scattering at high photon virtualities Q^2 for the first time allows a partonic content of the Pomeron, a central object in diffractive physics deeply related to QCD vacuum, to be probed. Using these diffractive parton densities (DPDF) to predict various final states in ep and also in pp diffraction relies on collinear factorisation theorem [1] and hence provides crucial tests of major concepts and overall consistency of QCD picture of diffraction in high energy particle collisions.

Leading order diagram for diffractive DIS together with the basic kinematic variables is shown in Fig. 1. Experimentally, events of such class can be detected by two complementary methods: either by direct observation of scattered proton in the apparatus located far from the interaction region close to the beampipe (p -tag), or by presence of non-exponentially suppressed large rapidity gaps void of any particle activity (LRG). In the latter case in addition to ‘elastic’ diffraction data contain some admixture of proton dissociation, typically with low mass M_X .

Below, four new measurements are presented, performed by the H1 and ZEUS collaborations, which benefit from large integrated luminosity, or from the detector upgrades implemented for HERA2 running period (2004-2007).

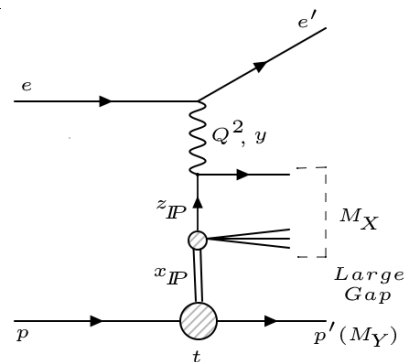


Figure 1: Born level diagram for diffractive deep-inelastic scattering $ep \rightarrow e' X p'$. Standard DIS variables: photon virtuality Q^2 and inelasticity y define kinematics at the lepton vertex, while two additional variables: $x_{\mathbb{P}}$ and t - the longitudinal momentum fraction of the incoming proton carried by the Pomeron and the four-momentum transfer squared at the proton vertex, respectively - describe the kinematics of diffractive exchange. $z_{\mathbb{P}} = x_{Bj}/x_{\mathbb{P}}$ represents the fractional longitudinal momentum of the Pomeron transferred to hard subprocess. Event topology exhibits large gap in rapidity separating M_X and M_Y systems.

2. Isolated photons in diffractive photoproduction

Prompt photons in diffractive events are interesting in two respects. First, they are direct messengers from hard subprocess which, unlike jets, are not affected by fragmentation. In addition, photons couple to charged partons only and hence they probe quark content of the Pomeron in diffractive processes. Here first preliminary results on this subject obtained by ZEUS Collaboration [2] are presented. Using two data samples of 91 pb^{-1} (HERA1) and 374 pb^{-1} (HERA2) respectively, high transverse energy photons $4 < E_T^\gamma < 15 \text{ GeV}$ are selected in central pseudo-rapidity range $-0.7 < \eta^\gamma < 0.9$ in diffractive photoproduction: $Q^2 < 1 \text{ GeV}^2$, $0.2 < y < 0.7$, $x_P < 0.03$. In $\sim 85\%$ of such events an isolated photon is accompanied by a jet with $E_T^{\text{Jet}} > 4 \text{ GeV}$. A template fit of the energy weighted cluster width is employed to statistically separate signal and background originating mainly from π^0 and η decays. The dominant systematic uncertainty, $\pm 22\%$, is related to LRG signature and estimation of the non-diffractive background. Further sources contribute to overall normalisation uncertainty of $\pm 25\%$.

The data are corrected to the hadron level and compared with theory as provided by the Rapgap MC program [3], normalised to the data. A $80 : 20$ mixture of *direct* ($x_\gamma = 1$) and *resolved* ($x_\gamma < 1$) components, where x_γ is a fraction of incoming photon energy participating in hard subprocess, gives a reasonable description of the data (Fig. 2a). In Fig. 2b the cross section is given as a function of z_P . The data show prominent peak at largest z_P which is not expected and not reproduced by the Rapgap. All other distributions are well described by this model. Note, that DPDFs [4] used in the Rapgap program are not well constrained at large z_P , hence these data could potentially be used to improve the precision of DPDF in this corner of the phase space.

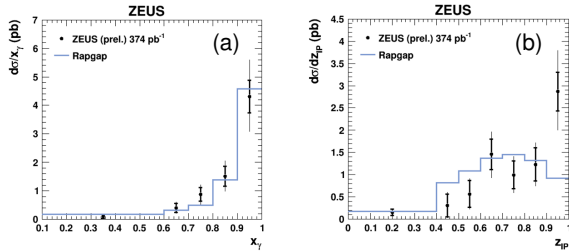


Figure 2: Differential cross section as a function of x_γ (a) and of z_P (b), for diffractive events containing an isolated photon and a jet, compared to normalised prediction from Rapgap MC.

3. D^* in diffractive DIS

Contrary to prompt photons, charm in diffractive ep scattering is produced predominantly via boson-gluon fusion, and thus is strongly sensitive to the gluon content of the Pomeron. D^* mesons reconstructed via so called ‘golden’ decay mode $D^{*+} \rightarrow D^0 \pi_{\text{slow}}^+ \rightarrow (K^- \pi^+) \pi_{\text{slow}}^+ + C.C.$ provide a convenient way of tagging open charm production. H1 Collaboration has used 281 pb^{-1} data sample, representing 6-fold increase as compared to previously published result, to measure D^* cross section in diffractive DIS [5] for $p_{T,D^*} < 1.5 \text{ GeV}$ and $-1.5 < \eta_{D^*} < 1.5$ in the range of $5 < Q^2 < 100 \text{ GeV}^2$ and inelasticity $0.02 < y < 0.65$. Diffractive events are selected using LRG signature and correspond to the following phase space: $x_P < 0.03$, $|t| < 1 \text{ GeV}^2$ and $M_Y < 1.6 \text{ GeV}$.

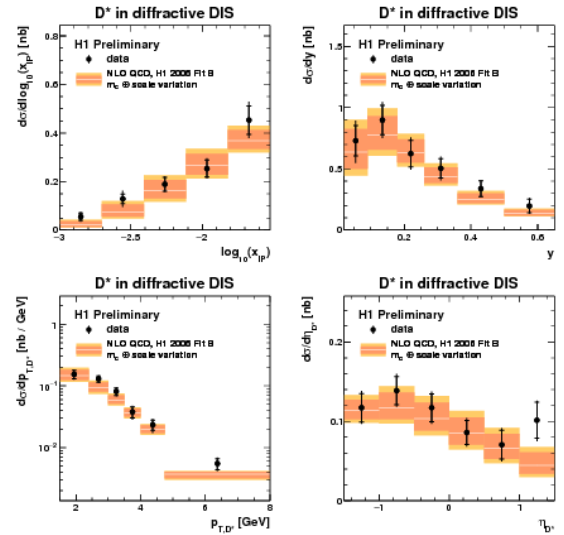


Figure 3: D^* meson cross sections as a function of the momentum fraction x_P , the inelasticity y , the D^* transverse momentum p_{T,D^*} and the D^* pseudorapidity η_{D^*} , compared to NLO QCD prediction.

In Fig. 3 the measured differential cross sections are confronted with the NLO QCD calculations [7] which use DPDF set [4] as determined in H1 inclusive diffraction and $\mu_r^2 = \mu_f^2 = m_c^2 + Q^2$ scale choice. For $c \rightarrow D^*$ fragmentation the Kartvelishvili parametrisation is used with the parameters fixed by the H1 inclusive D^* measurements [6]. Except of the forward region, $\eta_{D^*} > 1$, NLO QCD describes the data fairly well both in shapes and in absolute normalisation. This supports the universality of charm fragmentation and the QCD factorisation ansatz in diffractive DIS.

4. Ratio $\sigma_{\psi(2S)}/\sigma_{J/\psi(1S)}$ in exclusive DIS

An important testing ground for theoretical concepts and quantitative calculations in diffraction is provided by the study of exclusive vector meson (VM) production at HERA $e + p \rightarrow e + V + Y$. The exclusive deep inelastic electroproduction of $\psi(2S)$ and $J/\psi(1S)$ has been studied with the ZEUS detector in the kinematic range $2 < Q^2 < 80 \text{ GeV}^2$, $30 < W < 210 \text{ GeV}$ and $|t| < 1 \text{ GeV}^2$ [8]. Here the hard scale is given by both Q^2 and the mass of charm quark. Since these two charmonium states have same quark content, but different radial distributions of the wave functions (*w.f.*), their cross section ratio allows QCD predictions of the *w.f.* dependence on the $\bar{c}c$ -proton cross section to be tested. In particular, a suppression of $\psi(2S)$ relative to $J/\psi(1S)$ is expected due to the node in the $\psi(2S)$ *w.f.* leading to the destructive interference of the contributions from small and large $\bar{c}c$ dipoles to the production amplitude.

Since the reactions studied are statistically limited all available data have been used, amounting to 468 pb^{-1} . Moreover, in addition to the $\mu^+\mu^-$ decay channels used for both VM's, the $\psi(2S) \rightarrow J/\psi(1S)\pi^+\pi^-$ decay was exploited as well. The final sample contains ~ 2500 $J/\psi(1S)$ and ~ 190 $\psi(2S)$ events. After correcting for the detector acceptance, efficiency and the branching ratios, the cross section ratio $R = \sigma_{\psi(2S)}/\sigma_{J/\psi(1S)}$ was determined in bins of Q^2 , W and $|t|$ with statistical precision of $\sim 20\%$ and systematic uncertainty $\sim 10\%$. While as a function of W and $|t|$ the values of R are found to be compatible with a constant, the Q^2 dependence shows a positive slope with the significance of $\sim 2.5\sigma$.

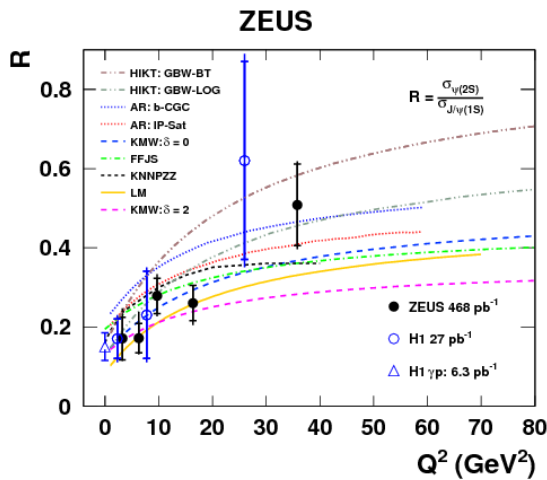


Figure 4: The cross-section ratio $R = \sigma_{\psi(2S)}/\sigma_{J/\psi(1S)}$ as a function of Q^2 . HERA measurements are compared to different QCD model predictions.

In Fig. 4 the results are compared to the previous H1 measurements [9] and confronted with a set of QCD models [10]. One can see, that all models correctly predict the suppression strength at $Q^2 = 0$ and qualitatively reproduce the rise of R with Q^2 , however with a large spread in its magnitude. Thus, the experimental data, albeit with relatively large uncertainties, show a definite discriminating power which allows to disfavour some extreme model predictions.

5. Exclusive ρ^0 production with a leading neutron

Measurements of leading baryon production in high energy particle collisions provide important inputs for the theoretical understanding of strong interactions in the soft, non-perturbative regime. The aim of the analysis presented here is to investigate exclusive ρ^0 production on virtual pions in the photoproduction regime at HERA and to extract for the first time experimentally the quasi-elastic $\gamma\pi \rightarrow \rho^0\pi$ cross section. Since no hard scale is present a phenomenological approach, such as Regge theory [12], is most appropriate to describe the reaction. Fig. 5 gives a set of Regge diagrams [13, 14] contributing to the signal (a,b,c) and to the background (d) for this process, where the pion exchange graph (a) is of prime interest. This one-pion-exchange (OPE) diagram dominates at small $t \rightarrow 0$, where the graphs 5b and 5c contributing to the scattering amplitude with opposite signs largely cancel.

In the OPE approximation the cross section of the reaction $\gamma + p \rightarrow \rho^0 + n + \pi^+$ can be presented as a pion flux convoluted with a photon-pion cross section

$$\frac{d^2\sigma_{\gamma p}(W_{\gamma p}, x_L, t)}{dx_L dt} = f_{\pi/p}(x_L, t) \sigma_{\gamma\pi}(W_{\gamma\pi}) \quad (1)$$

with the generic form of the pion flux factor [17]:

$$f_{\pi/p}(x_L, t) = \frac{1}{2\pi} \frac{g_{p\pi n}^2}{4\pi} (1 - x_L)^\beta \frac{-t}{(m_\pi^2 - t)^2} F^2(t, x_L) \quad (2)$$

Here $\beta = \alpha_P(0) - 2\alpha_\pi(t)$, $\alpha_P(0)$ is the Pomeron intercept, $\alpha_\pi(t) = \alpha'_\pi(t - m_\pi^2)$ is the pion trajectory, $g_{p\pi n}^2/4\pi$ is the $p\pi n$ coupling constant known from phenomenological analysis of low energy data, and $F(t, x_L)$ is a form factor accounting for off mass-shell corrections and normalised to unity at the pion pole, $F(m_\pi^2, x_L) = 1$. For exact definition of kinematic variables in eq. (1-2) see [16].

The analysis is based on ~ 6600 events, containing only two charged pions from ρ^0 decay and a leading neutron with energy $E_n > 120 \text{ GeV}$, and nothing else

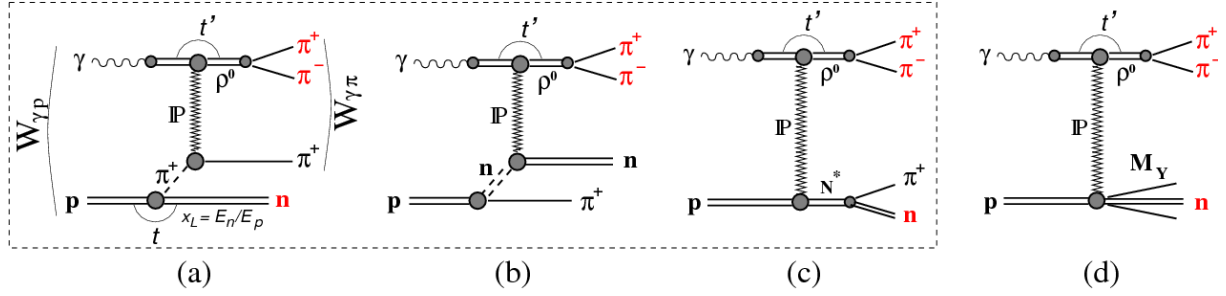


Figure 5: Generic diagrams for processes contributing to exclusive photoproduction of ρ^0 mesons associated with leading neutrons at HERA. The signal corresponds to the Drell-Hiida-Deck model graphs for the pion exchange (a), neutron exchange (b) and direct pole (c). Diffractive scattering in which a neutron may be produced as a part of the proton dissociation system, M_Y , contributes as background (d). The N^* in (c) denotes both resonant (via N^+) and possible non-resonant $n + \pi^+$ production.

above noise level in the detector. This ensures the exclusivity and limits the dissociative background to the range $M_Y < 1.6$ GeV. The sample corresponds to an integrated luminosity of 1.16 pb^{-1} , collected by a special minimum bias track trigger in the years 2006-2007 at $\sqrt{s_{ep}} = 319$ GeV. Diffractive dissociation background is modelled by the Diffvm program [15] and statistically separated from the signal, $\gamma p \rightarrow \rho^0 n \pi^+$, on the basis of the neutron energy distribution shape. It amounts to $(34 \pm 5)\%$ and gives the dominant experimental uncertainty to the cross section measurement. Further details of the analysis can be found in [16].

The cross sections for the reaction $\gamma p \rightarrow \rho^0 n \pi^+$ are measured for two ranges of the neutron transverse momentum, $p_{T,n}$: $p_{T,n} < 0.69 E_n$, corresponding to the full angular acceptance of the neutron calorimeter, $\theta_n < 0.75$ mrad, and for so called OPE safe range, $p_{T,n} < 0.2$ GeV.

In Fig. 6 the data are compared to the predictions, based on different models for the pion flux [17]. The shape of x_L distribution is described by most of the models, although some of them can be ruled out already at that level (Fig. 6a). Additional constraints on the pion flux models could be provided by the dependence on t (or $p_{T,n}^2$) of the leading neutron. The x_L dependence of the measured exponential slopes, $b_n(x_L)$, of the double differential cross section $d^2\sigma_{\gamma p}/dx_L dp_{T,n}^2$ is shown on Fig. 6d. Despite of the large experimental uncertainties none of the models is able to reproduce the data. A possible explanation [14, 18] could be absorptive corrections which modify the t dependence of the amplitude, leading to an increase of the effective b -slope at large x_L as compared to the pure OPE model without absorption.

The pion flux models compatible with the data in shape of the x_L distribution are used to extract the photon-pion cross section from $d\sigma/dx_L$ in the OPE ap-

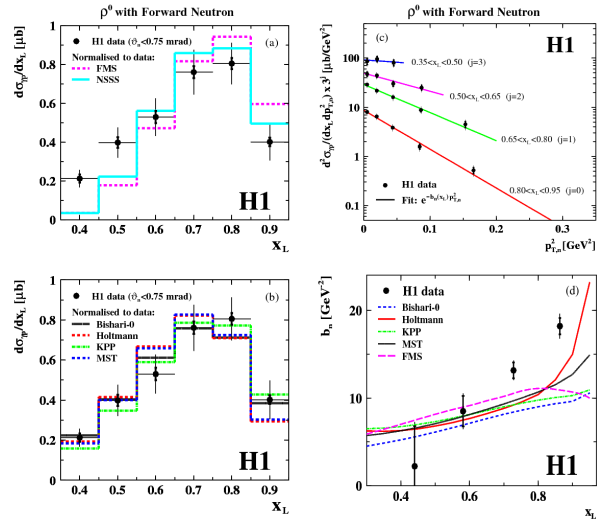


Figure 6: (a,b) Differential cross section $d\sigma_{\gamma p}/dx_L$ in the range $20 < W_{\gamma p} < 100$ GeV compared to the predictions based on different versions of pion fluxes. (c) Double differential cross section $d^2\sigma_{\gamma p}/dx_L dp_{T,n}^2$ fitted with single exponential functions. The cross sections in different x_L bins j are scaled by the factor 3^j for better visibility. (d) The exponential slopes fitted through the $p_{T,n}^2$ dependence of the leading neutrons as a function of x_L . The data points are compared to the expectations of several parametrisations of the pion flux within the OPE model.

proximation:

$$\sigma(\gamma\pi^+ \rightarrow \rho^0\pi^+) = 2.33 \pm 0.34 (\text{exp})_{-0.40}^{+0.47} (\text{model}) \mu\text{b},$$

where the experimental uncertainty includes statistical, systematic and normalisation errors added in quadrature, while the model error is due to the uncertainty in the pion flux integral obtained for the different flux parametrisations compatible with the data. Taking a value of $\sigma(\gamma p \rightarrow \rho^0 p) = (9.5 \pm 0.5) \mu\text{b}$ at the corresponding energy $\langle W \rangle = 24$ GeV, which is an interpola-

tion between fixed target and HERA measurements, one obtains for the ratio $r_{\text{el}} = \sigma_{\text{el}}^{\gamma\pi} / \sigma_{\text{el}}^{\gamma p} = 0.25 \pm 0.06$. A similar ratio, but for the total cross sections at $\langle W \rangle = 107$ GeV, has been estimated by the ZEUS collaboration as $r_{\text{tot}} = \sigma_{\text{tot}}^{\gamma\pi} / \sigma_{\text{tot}}^{\gamma p} = 0.32 \pm 0.03$ [20]. Both ratios are significantly smaller than their respective expectations, based on simple considerations. For r_{tot} , a value of $2/3$ is predicted by the additive quark model, while $r_{\text{el}} = \left(\frac{b_{\gamma p}}{b_{\gamma\pi}}\right) \cdot (\sigma_{\text{tot}}^{\gamma\pi} / \sigma_{\text{tot}}^{\gamma p})^2 = 0.57 \pm 0.03$ can be deduced by combining the optical theorem, the eikonal approach relating cross sections with elastic slope parameters and the data on pp, π^+p and γp elastic scattering. Such a suppression of the cross section is usually attributed to rescattering, or absorptive corrections [18, 19], which are essential for leading neutron production. For the exclusive reaction $\gamma p \rightarrow \rho^0 n \pi^+$ studied here this would imply an absorption factor of $K_{\text{abs}} = 0.44 \pm 0.11$.

Finally, the cross section as a function of the four-momentum transfer squared of the ρ^0 meson, t' , is presented in Fig. 7. It exhibits the very pronounced feature of a strongly changing slope between the low- t' and the high- t' regions, which is characteristic to double peripheral exclusive reactions. In the DHD model it is a consequence of the interference between the amplitudes corresponding to the diagrams *a*, *b* and *c* in Fig. 5. In a geometric picture, the large value of slope b_1 suggests that for a significant part of the data ρ^0 mesons are produced at large impact parameter values of order $\langle r^2 \rangle = 2b_1 \cdot (\hbar c)^2 \approx 2\text{fm}^2 \approx (1.6R_p)^2$.

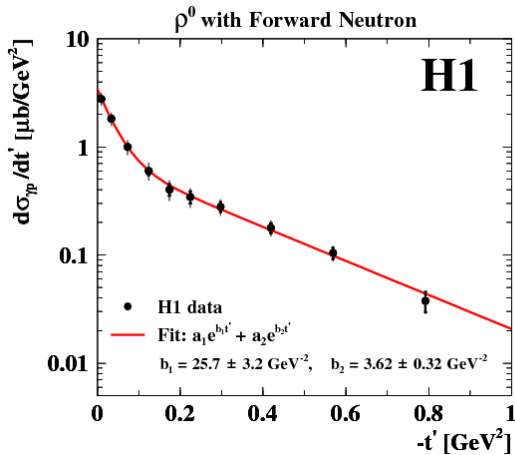


Figure 7: Differential cross section $d\sigma_{\gamma p}/dt'$ of ρ^0 mesons fitted with the sum of two exponential functions. The inner error bars represent statistical and uncorrelated systematic uncertainties added in quadrature and the outer error bars are total uncertainties, excluding an overall normalisation error of 4.4%. The values of slopes are characteristic for double peripheral processes in which an exchange of two Regge trajectories is involved.

6. Summary

Four new measurements are presented in the area of diffractive and exclusive channels, by the H1 and ZEUS collaborations, making use of full HERA data samples. Whenever hard scale is present, pQCD calculations are successful. The data show sensitivity to some QCD models parameters. They can also be used to further constrain DPDFs, especially at high z_P . Photon-pion elastic cross section is extracted for the first time experimentally in the one-pion-exchange approximation. Strong absorptive effects are confirmed in leading neutron production. Since the nature of those is non-perturbative, new experimental results are essential for the tuning of ‘Survival Gap Probability’ models.

References

- [1] J. C. Collins, *Phys. Rev.* **D57** (1998) 3051. Erratum-ibid. 61, 019902 (2000).
- [2] ZEUS Collaboration, ZEUS-prel-15-001 (2015).
- [3] H. Jung, *Comp. Phys. Commun.* **86** (1995) 147.
- [4] A. Aktas *et al.* [H1 Collab.], *Eur. Phys. J.* **C48** (2006) 715.
- [5] H1 Collaboration, H1prelim-16-011 (2016).
- [6] F.D. Aaron *et al.* [H1 Collab.], *Eur. Phys. J.* **C59** (2009) 589; F.D. Aaron *et al.* [H1 Collab.], *Eur. Phys. J.* **C71** (2011) 1769.
- [7] B.W. Harris and J. Smith, *Phys. Rev.* **D57** (1998) 2806.
- [8] H. Abramowicz *et al.* [ZEUS Collab.], [arXiv:1606.08652]
- [9] C. Adloff *et al.* [H1 Collab.], *Phys. Lett.* **B421** (1998) 385; C. Adloff *et al.* [H1 Collab.], *Eur. Phys. J.* **C10** (1999) 373.
- [10] See ref. [33 – 40, 45 – 49] in [8].
- [11] N.F. Bali, G.F. Chew and A. Pignotti, *Phys. Rev. Lett.* **19** (1967) 614; G.F. Chew and A. Pignotti, *Phys. Rev.* **176** (1968) 2112; E.L. Berger, *Phys. Rev.* **179** (1969) 1567.
- [12] P. D. B. Collins, “*An Introduction to Regge Theory and High-Energy Physics*”, Cambridge University Press, 1977.
- [13] S.D. Drell and K. Hiida, *Phys. Rev. Lett.* **7** (1961) 199; R.T. Deck, *Phys. Rev. Lett.* **13** (1964) 169; F. Hayot *et al.*, *Lett. Nuovo Cim.* **18** (1977) 185.
- [14] N.P. Zotov and V.A. Tsarev, *Sov. J. Part. Nucl.* **9** (1978) 266.
- [15] B. List and A. Mastroberardino, Proc. of the Workshop on Monte Carlo Generators for HERA Physics, eds. A.T. Doyle *et al.*, DESY-PROC-1999-02 (1999) 396.
- [16] V. Andreev *et al.* [H1 Collab.], *Eur. Phys. J.* **C76** (2016) 41.
- [17] (a) M. Bishari, *Phys. Lett.* **B38** (1972) 510; (b) H. Holtmann, A. Szczurek and J. Speth, *Nucl. Phys.* **A596** (1996) 631; M. Przybycien, A. Szczurek and G. Ingelman, *Z. Phys.* **C74** (1997) 509; (c) B. Kopeliovich, B. Povh and I. Potashnikova, *Z. Phys.* **C73** (1996) 125; (d) W. Melnitchouk, J. Speth and A.W. Thomas, *Phys. Rev.* **D59** (1999) 014033; (e) L. Frankfurt, L. Mankiewicz and M. Strikman, *Z. Phys.* **A334** (1989) 343; (f) N.N. Nikolaev, W. Schäfer, A. Szczurek and J. Speth, *Phys. Rev.* **D60** (1999) 014004.
- [18] A.B. Kaidalov *et al.*, *Eur. Phys. J.* **C47** (2006) 385; B.Z. Kopeliovich *et al.*, *Phys. Rev.* **D85** (2012) 114025.
- [19] N. Nikolaev, J. Speth and B.G. Zakharov, hep-ph/9708290; U. D’Alesio and H.J. Pirner, *Eur. Phys. J.* **A7** (2000) 109.
- [20] S. Chekanov *et al.* [ZEUS Collab.], *Nucl. Phys.* **B637** (2002) 3.